

and trans-reduced *syn*-sesquiorbornenes (or sesquiorbornanes), shown in Figure 15. As concluded above on the basis of non-bonded interaction, the endo-reduced species is considerably more stable than the exo.<sup>49</sup> Furthermore, the trans-bent species is so high in energy that the trans-bent triplet is clearly impossible for the *syn*-sesquiorbornene triplet.

The identification of pyramidalization without significant rotation of alkene triplets as a relaxation mechanism should bring new insight into the understanding of the transients formed in photochemistry of constrained species.<sup>50</sup>

(49) After submission of this manuscript, crystal structures of several derivatives of an exo-bent derivative of sesquiorbornene were reported: Ermer, O.; Mason, S. A. *J. Chem. Soc., Chem. Commun.* **1983**, 53. The nearest hydrogen-hydrogen contacts, corresponding to that between H<sub>11en</sub> and H<sub>12en</sub> in **2**, are 1.713 and 1.754 Å in two derivatives. CFF and MM2 force fields predict 0.14–0.13-Å larger separation.

(50) See, for example, Bonneau, R. *J. Am. Chem. Soc.* **1980**, *102*, 3816. Bonneau, R.; Jousset-Dubien, J.; Salem, L.; Yarwood, A. J. *Ibid.* **1976**, *98*, 4329. Dauben, W. G.; van Riel, H. C. H. A.; Hauw, C.; Leroy, F.; Jousset-Dubien, J.; Bonneau, R. *Ibid.* **1979**, *101*, 1901. Dauben, W. G.; van Riel, H. C. H. A.; Robbins, J. D.; Wagner, G. J. *Ibid.* **1979**, *101*, 6383. Bonneau, R.; Jousset-Dubien, J.; Yarwood, J.; Pereyre, J. *Tetrahedron Lett.* **1977**, 235.

(51) Note Added in Proof: Optimization of the *syn*-sesquiorbornene triplet at the UHF STO-3G level with CH lengths fixed at 1.09 Å gives two minima, an exo-bent (by 44°) species and an endo-bent (by 32°) species which is 10.3 kcal/mol higher in energy.

(52) Note Added in Proof: A pyramidal *anti*-sesquiorbornene structure has been identified by X-ray crystallography: Ermer, O.; Bödecker, C.-D. *Helv. Chim. Acta* **1983**, *66*, 943. This is consistent with the easy deformation of the *anti*-2 sesquiorbornene predicted by MM2.

## Conclusions

*syn*-Sesquiorbornene, like norbornene, is pyramidalized to minimize torsional repulsions between alkene carbon orbitals and allylic bond orbitals. This pyramidalization causes tiny increases in the exo HOMO extension owing to both antibonding interactions with allylic endo  $\sigma$  orbitals and to sp mixing, but the outward tilting on the exo face is a more significant effect. Thermal exo additions occur to minimize torsional strain between the forming bonds and allylic bonds. Triplets of small ring alkenes pyramidalize nearly to sp<sup>3</sup> geometries. Both trans and cis isomers are formed, separated by a small barrier. *syn*-Sesquiorbornene can significantly pyramidalize only in an exo fashion, so only endo photoreduction is observed.

**Acknowledgment.** We are grateful to Professors Paul D. Bartlett, William H. Watson, and Kenneth D. Jordan for helpful discussions, to Professor John A. Pople and Michael Frisch for the use of Gaussian 80 and 82 and the Carnegie-Mellon VAX and ARCHIVE, and to the National Science Foundation and donors of the Petroleum Research Fund, administered by the American Chemical Society, for financial support of this research. A U.S. Senior Scientist Award to K.N.H. from the Alexander von Humboldt Foundation, and encouragement, hospitality, and helpful comments by Professor Paul van Ragué Schleyer made completion of this work possible.

**Registry No.** *syn*-Sesquiorbornene, 73321-28-5; *anti*-sesquiorbornene, 73679-39-7.

## Intramolecular Excimer Emission of Poly(*N*-vinylcarbazole) and *rac*- and *meso*-2,4-Di-*N*-carbazolylpentane. Model Substances for Its Syndiotactic and Isotactic Dyads

F. Evers,<sup>†</sup> K. Kobs, R. Memming,\* and D. R. Terrell<sup>‡</sup>

Contribution from the Philips GmbH, Forschungslaboratorium Hamburg, D-2000 Hamburg 54, West Germany. Received January 20, 1983

**Abstract:** The dimeric model compounds for isotactic and syndiotactic poly(*N*-vinylcarbazole) (PVK), *meso*- and *rac*-2,4-di-*N*-carbazolylpentane, have been prepared and have been found to exhibit the typical carbazole monomer emission together with excimer emission characteristic for each isomer. These meso and racemic excimer emission bands have been correlated with the 420- and 370-nm excimer emission bands found in PVK. New insight in the nature and formation of excimer states was obtained by additional studies of the steric microstructure of PVK. Data of the fluorescence kinetics, of NMR, and of the glass transition temperatures gave evidence that the 420- and 370-nm excimer emission bands derive independently from isotactic and syndiotactic PVK diads.

The photophysical properties of poly(*N*-vinylcarbazole) (PVK) have been the subject of intense study, partly with a view to gaining an insight into its photoconductive properties<sup>1</sup> and partly due to its unique photophysical properties. In contrast to other aromatic-containing polymers, no fluorescence emission from monomer-like moieties has been observed.<sup>2,3</sup> In solution the broad unstructured fluorescence is resolved into two peaks, which have been assigned to two spectrally distinct excimer species.<sup>3-6</sup> One of these, with a  $\lambda_{\max}$  of 420 nm, has been attributed to a "sandwich-type" excimer formed between neighboring carbazole groups on the polymer chain in a totally eclipsed conformation<sup>3</sup>

and the other, with a  $\lambda_{\max}$  of 380 nm, has been less well characterized, although Johnson<sup>3</sup> has suggested a dimeric structure, with considerable deviation from coplanarity, of the carbazole rings. Itaya et al.,<sup>6</sup> on the other hand, have proposed a structure with only one eclipsed aromatic ring from each group.

(1) Penwell, R. C.; Ganguly, B. N.; Smith, T. W. *Macromol. Rev.* **1978**, *13*, 63.

(2) Kloeppfer, W. *J. Chem. Phys.* **1969**, *50*, 2337.

(3) Johnson, G. E. *J. Chem. Phys.* **1975**, *62*, 4697.

(4) Ghiggino, K. P.; Wright, R. D.; Phillips, D. *Eur. Polym. J.* **1978**, *14*, 567.

(5) Hoyle, C. E.; Et al. *Macromolecules* **1978**, *11*, 429.

(6) Itaya, A.; Okamoto, K.; Kusabayashi, S. *Bull. Chem. Soc. Jpn.* **1976**, *49*, 2082.

<sup>†</sup> Present address: Hermal-Chemie, Hamburg.

<sup>‡</sup> Present address: Agfa-Gevaert N.V., R&D Laboratories, B-2510 Mortsel, Belgium.

Table I. <sup>1</sup>H NMR Data of Diastereoisomers of 2,4-Dis-*N*-carbazolypentane

$\delta$	multiplicity	group of protons
<i>meso</i> -BCPe		
1.59	d	CH <sub>3</sub>
2.73 (A)	2 sextuplets	H <sub>A</sub> CH <sub>B</sub>
2.91 (B)		
4.53	sextuplet	CH
7.1-8.2	m	carbazolyl
<i>rac</i> -BCPe		
1.48	d	CH <sub>3</sub>
3.13	sextuplet	CH <sub>2</sub>
4.46	sextuplet	CH
7.1-8.2	m	carbazolyl

Often additional insight into the fluorescence emission of a polymer can be obtained by examining the fluorescence emission of low molecular weight model substances. Indeed studies of the fluorescence emission spectra of 1,3-di-*N*-carbazolylpropane have shown the presence of both monomer fluorescence and a broad structureless peak at lower energy assigned to a sandwich-type excimer.<sup>7-9</sup> In the absence of the steric constraints present in the analogous polymer the excimer formed would be expected to be the lower energy excimer, as is in fact observed. It was therefore thought worthwhile to synthesize model substances in which the carbazole substituents would be subject to the same constraints as in the polymer chain. The simplest molecules that satisfy this aim are *rac*- and *meso*-2,4-di-*N*-carbazolypentane (BCPe), which correspond in PVK to the syndiotactic and isotactic diads, respectively.

This paper describes the synthesis and fluorescence emission properties of *rac*- and *meso*-BCPe, together with the kinetics of their excimer emissions. The fluorescence emission spectra of *rac*- and *meso*-BCPe have been previously published in a preliminary publication<sup>10</sup> and have also been reported recently by De Schryver et al.<sup>11</sup>

The fluorescence emission spectra of these model substances were used, in combination with the fluorescence emission spectra of PVK samples with different steric microstructures,<sup>12-14</sup> to obtain an insight into the fluorescence emission of PVK. Indeed the suggestion made by De Schryver et al.<sup>11</sup> that the excimer emission spectra of *rac*- and *meso*-BCPe are related to the two excimers observed in PVK is confirmed, a correlation being found between the peak area ratio of the two excimers for a series of PVK samples and their isotactic:syndiotactic dyad ratios from the methine peaks in the <sup>13</sup>C NMR spectrum of PVK.

## Results and Discussion

**Synthesis of *rac*- and *meso*-BCPe.** The synthesis of *rac*- and *meso*-BCPe proved to be very difficult, since direct substitution of the tosyloxy groups in 2,4-ditosyloxy-pentane (DTPe) by carbazolyl groups using sodium carbazole in Me<sub>2</sub>SO at room temperature produced exclusively *meso*-BCPe together with the elimination product 4-*N*-carbazolypent-2-ene. This was confirmed by the 270-MHz <sup>1</sup>H NMR spectrum, the double sextuplet for the methylene group being indicative of the two methylene protons experiencing different environments and hence of a *meso* structure. Furthermore the addition of chiral shift reagents was found to have no effect upon the <sup>1</sup>H NMR spectrum.

Since *rac*-BCPe could not be prepared by direct substitution, the syntheses of precursors that could be connected to BCPe, but that were less sterically crowded, were investigated. Morgan et

Table II. <sup>13</sup>C NMR Data of Diastereoisomers of 2,4-Dis-*N*-carbazolypentane

$\delta$		carbon atom
<i>meso</i> -BCPe	<i>rac</i> -BCPe	
18.80	19.19	CH <sub>3</sub>
40.37	39.58	CH <sub>2</sub>
48.90	48.93	CH
110.41	110.41	aromatic
119.16	119.22	
120.61	120.63	
123.97	124.02	
125.71	125.81	
140.14	140.15	

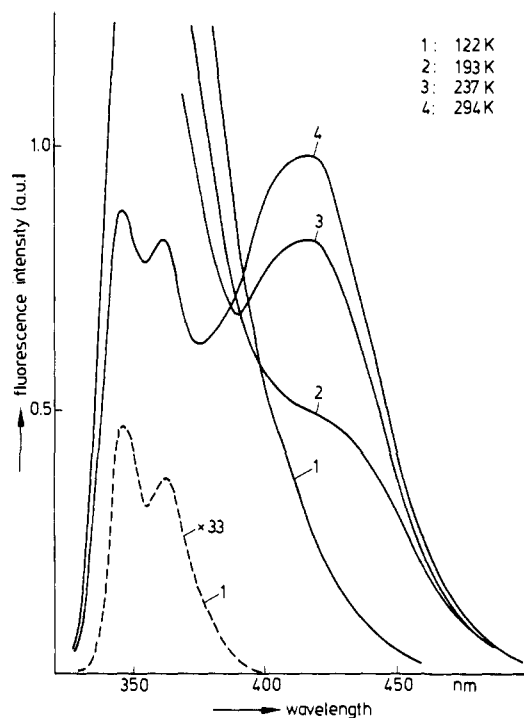


Figure 1. Emission spectra of *meso*-BCPe in deaerated solutions of methylcyclohexane/isopentane (1:1) (MCH/ISP) at various temperatures. concn =  $9 \times 10^{-6}$  M.

al.<sup>15</sup> had reported that a mixture of *rac*- and *meso*-2,3-dianilinobutane could be prepared by heating aniline and 2,3-dibromobutane together at 160 °C for 4 h. The reactions of various amines with DTPe at 160 °C were therefore investigated. It was found that 1,2,3,4-tetrahydrocarbazole (THC) did not react, but that freshly distilled aniline and freshly prepared 1,2,3,4,10,11-hexahydrocarbazole (HHC) reacted with DTPe to produce mixtures of *rac*- and *meso*-2,4-dianilinopentane and *rac*- and *meso*-2,4-di-*N*-1,2,3,4,10,11-hexahydrocarbazolypentane (BHHCPe), respectively. This reaction appeared to depend upon the basicity of the amine used, since HHC has a similar basicity to aniline, whereas the aromatization of the pyrrole ring in THC would considerably reduce the basicity of the amino group. Finally BHHCPe was dehydrated to BCPe by refluxing with chloranil in xylene.<sup>16</sup>

**NMR Spectra of *rac*- and *meso*-BCPe.** De Schryver et al.<sup>11</sup> have published <sup>1</sup>H NMR spectra of impure *rac*- and *meso*-BCPe. <sup>1</sup>H NMR data for the pure diastereoisomers of BCPe in deuteriochloroform at room temperature and 1,2-dibromoethane-*d*<sub>4</sub> at 110 °C for *meso*-BCPe and *rac*-BCPe, respectively, obtained on a 270-MHz Bruker spectrometer are given in Table I. An interesting feature of the <sup>1</sup>H NMR spectrum of *rac*-BCPe is that the aromatic protons exhibit very broad peaks at room temper-

- (7) Kloepffer, W. *Chem. Phys. Lett.* **1969**, *4*, 193.  
 (8) Johnson, G. E. *J. Chem. Phys.* **1974**, *61*, 3002.  
 (9) Johnson, G. E. *J. Chem. Phys.* **1975**, *63*, 4047.  
 (10) Terrell, D. R., poster at "Polymerization Mechanisms Symposium", Liverpool University (U.K.), Sept 1980.  
 (11) De Schryver, F. C.; Vandendriessche, J.; Toppet, S.; Demeyer, K.; Boens, N. *Macromolecules* **1982**, *15*, 406.  
 (12) Terrell, D. R.; Evers, F. *Makromol. Chem.* **1982**, *183*, 863.  
 (13) Terrell, D. R. *Polymer* **1982**, *23*, 1045.  
 (14) Terrell, D. R.; Evers, F. *J. Polym. Sci., Part A-1* **1982**, *20*, 2529.

- (15) Morgan, G. T.; Skinner, D. G. *J. Chem. Soc.* **1925**, *127*, 1731.  
 (16) Barclay, B. M.; Campbell, N. *J. Chem. Soc.* **1945**, 530.

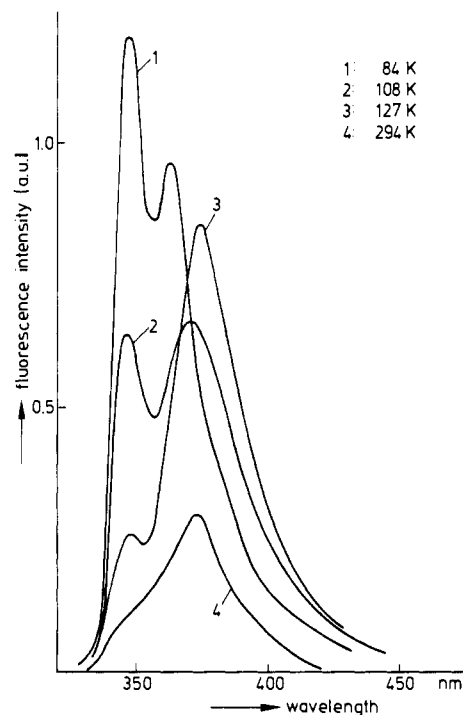


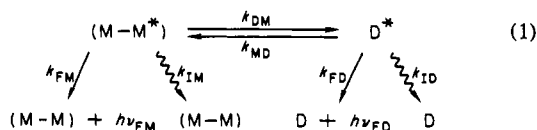
**Figure 2.** Emission spectra of *rac*-BCPe in deaerated solutions of MCH/ISP at various temperatures. concn =  $8.5 \times 10^{-6}$  M.

ature. This peak broadening can be removed by running the  $^1\text{H}$  NMR spectrum at higher temperatures. Thus at 110 °C in 1,2-dibromoethane- $d_4$  the peak broadening has completely disappeared. This effect is indicative of severe steric hindrance in *rac*-BCPe, which is consistent with the absence of *rac*-BCPe upon direct substitution of the tosyloxy groups in DTpe by carbazolyl groups using sodium carbazole in  $\text{Me}_2\text{SO}$  at room temperature. The chemical shifts for the two methylene protons in *meso*-BCPe differed by 0.18 ppm as compared with 0.21 ppm in *meso*-2,4-diphenylpentane.<sup>17</sup>

$^{13}\text{C}$  NMR data for the pure diastereoisomers of BCPe in dioxane solution at 60 °C are given in Table II.

**Kinetics of Excimer Formation in *rac*- and *meso*-BCPe.** As reported by Terrell<sup>10</sup> and more recently by De Schryver<sup>11</sup> the fluorescence emission spectra of *rac*- and *meso*-BCPe exhibit very different habits, as shown in Figures 1 and 2. These measurements were performed in deaerated solutions to avoid oxygen quenching of the emission. The *meso* diastereoisomer exhibits an excimer emission at ca. 430 nm, whereas the *racemic* diastereoisomer exhibits an excimer emission at ca. 375 nm.

The kinetics of excimer formation for the two diastereoisomers was studied in detail. The reaction mechanism is described by the usual scheme (eq 1). The notation is that of Birks.<sup>18</sup> Under



photostationary conditions the intensity of the excimer emission ( $I_E$ ) is given by

$$\frac{1}{I_E} = \frac{k_M}{k_{DM}}(k_D + k_{MD}) + k_D \frac{1}{gk_{FD}} \quad (2)$$

in which  $k_M = k_{FM} + k_{IM}$ ,  $k_D = k_{FD} + k_{ID}$ , and  $g$  is the rate of

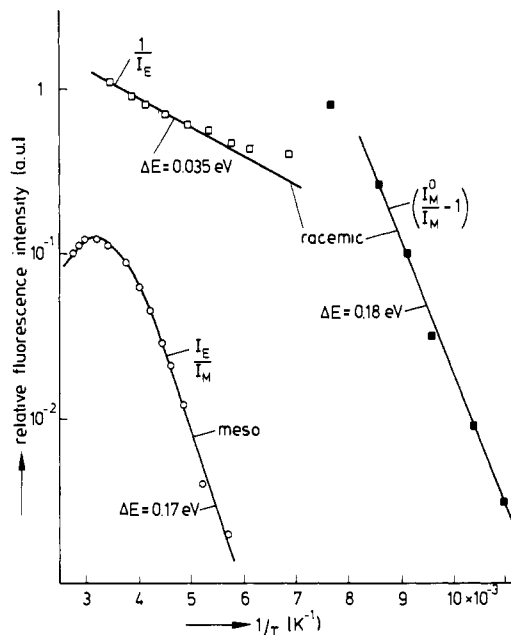


**Figure 3.** Relative emission intensities of *meso*- and *rac*-BCPe vs. reciprocal temperature in deaerated solutions of MCH/ISP.

excitation of the monomers. The monomer emission  $I_M$  is given by

$$\frac{I_M^\infty}{I_M} - 1 = \frac{k_D k_{DM}}{k_M(k_D + k_{MD})} \quad (3)$$

in which  $I_M = I_M^\infty = g$  for  $k_{DM} = 0$ . Combining eq 2 and 3 we have

$$\frac{I_E}{I_M} = \frac{k_{DM}}{k_D + k_{MD}} \frac{k_{FD}}{k_{FM}} \quad (4)$$

In accordance with eq 4 the ratio of excimer and monomer emission was plotted against  $T^{-1}$  for the *meso* isomer in Figure 3. Such a plot was not possible for the *racemic* diastereoisomer owing to the strong overlap of the monomer and excimer emission (see Figure 2). However, the excimer and monomer emissions dominate at the extremes of the temperature range examined, which allows the plotting of  $1/I_E$  vs.  $T^{-1}$  in the high-temperature range (see eq 2) and  $(I_M^\infty/I_M - 1)$  vs.  $1/T$  in the low-temperature range (see eq 3).

According to eq 3 and 4 the negative gradient of the two curves in the low-temperature region yields the activation energy for the intramolecular excimer formation  $E_{DM}$ . We obtained a value of 0.17 eV for the *meso* and 0.18 eV for the *racemic* diastereoisomer. These values are similar in magnitude to barriers to rotational motion about carbon-carbon bonds in alkanes.<sup>8</sup>

In the high-temperature region (below the maximum) the excimer and monomer emissions are only determined by the ratio  $k_{DM}/k_{MD}$ ; i.e., the monomer and excimer are in equilibrium. Therefore the slope of the curves yields the difference in the activation energies representing the formation and dissociation of the excimer. A  $\Delta E = E_{MD} - E_{DM}$  of 0.035 eV was obtained for the *racemic* isomer and therefore  $E_{MD} = 0.21$  eV. Unfortunately the high-temperature range was too small for obtaining the corresponding value for the *meso* diastereoisomer. However, since the maximum in  $I_E/I_M$  in this case occurs at much higher temperatures than for the *racemic* isomer it is reasonable to assume that  $k_{MD}$  attains comparable values to  $k_D$  only in this temperature range. This indicates that the dissociation energy is considerably higher than for the *racemic* diastereoisomer. This deduction is further supported by the fact that the emission maximum of the *meso* excimer occurs at considerably longer wavelengths than that of the *racemic* excimer.

Further insight into the mechanism was sought by determining the rate constants using emission decay measurements. Solution

(17) Bovey, F. A. "High Resolution NMR of Macromolecules"; Academic Press: New York, 1972; pp 68-69.

(18) Birks, J. B. "Photophysics of Aromatic Molecules"; Wiley-Interscience: New York, 1970.

Table III

	$E_{DM}$ , eV	$E_{MD}$ , eV	$10^{-7}\lambda_1$ , $s^{-1}$	$10^7\lambda_2$ , $s^{-1}$	$10^{-7}k_M$ , $s^{-1}$	$10^{-7}k_D$ , $s^{-1}$	$10^{-7}k_{DM}$ , $s^{-1}$	$10^{-7}k_{MD}$ , $s^{-1}$
<i>meso</i> -BCPe	0.17	0.18	200	2.9	5.7	2.9	198	0.7
<i>rac</i> -BCPe	0.17	0.18			5.7			
ethylcarbazole					5.7			

of the rate equations appropriate to the kinetic scheme, given in eq 1, yields the following expressions for the time dependence of monomer and excimer fluorescence decays:<sup>18</sup>

$$I_M(t) = k_{FM}[A \exp(-\lambda_1 t) + B \exp(-\lambda_2 t)] \quad (5)$$

$$I_E(t) = \frac{k_{FD}k_{DM}}{\lambda_1 - \lambda_2} [\exp(-\lambda_2 t) - \exp(-\lambda_1 t)] \quad (6)$$

in which

$$A = -B = \frac{k_M + k_{DM} - \lambda_2}{\lambda_1 - \lambda_2}$$

$\lambda_{1,2} =$

$$\frac{1}{2}[(X + Y) \pm [(X + Y)^2 - 4(k_M k_D + k_D k_{DM} + k_M k_{MD})]^{1/2}]$$

$$X = k_M + k_D$$

$$Y = k_{DM} + k_{MD}$$

Our investigations were restricted to the *meso* isomer, because for an accurate determination it is necessary to have one wavelength at which only the monomer emits and one at which only the excimer emits. The emission of the racemic diastereoisomer exhibited too great an overlap of the monomer and excimer to enable an accurate determination of its rate constants. The results obtained with the *meso* diastereoisomer are given in Figures 4 and 5. The excimer emission yields a rise time of 0.4 ns, i.e.,  $\lambda_1 = 2.5 \times 10^9 s^{-1}$ , and a decay time of 35 ns, i.e.,  $\lambda_2 = 2.9 \times 10^7 s^{-1}$  at 295 K. This compares with 46.5 ns at 223 K and 34.9 ns at 350 K reported by De Schryver.<sup>11</sup> The monomer emission yields an essentially two-component decay. The fast decay time was 0.65 ns, i.e.,  $\lambda_1 = 1.5 \times 10^9 s^{-1}$ , and the long time range decay yielded a decay time of 33 ns, i.e.,  $\lambda_2 = 3.0 \times 10^7 s^{-1}$  at 295 K. Thus similar values were obtained from both measurements. The average of these values was used for further calculations, i.e.,  $\lambda_1 = 2.0 \times 10^9 s^{-1}$  and  $\lambda_2 = 2.9 \times 10^7 s^{-1}$ . The decay curve of the monomer emission also indicates a small trace of a third decay constant of ca. 13 ns, which we cannot explain. Since this does not occur in the excimer emission, we can only assume that it is due to the emission from carbazole monomers that do not form excimers.

With these data and eq 5 and 6 various rate constants were determined. Using  $k_M = 5.7 \times 10^9 s^{-1}$ , we obtained  $k_{DM} = 1.98 \times 10^9 s^{-1}$ , i.e., the first decay (represented by  $\lambda_1$ ) is almost entirely determined by  $k_{DM}$ . The other rate constants can only be derived if at least the sum  $k_D + k_{MD}$  is known. As discussed below, a value for this sum of  $3.6 \times 10^7 s^{-1}$  was obtained by quenching experiments. With this value and eq 5 and 6,  $k_D = 2.9 \times 10^7 s^{-1}$  and  $k_{MD} = 0.7 \times 10^7 s^{-1}$ . These data are summarized in Table III.

With regard to the nature of the two excimers, one obtains the best insight into their conformations by considering molecular models. In the case of the *meso* diastereoisomer the two chromophores exist in a sandwich-type configuration, as shown in Figure 6a, whereas in the case of the racemic diastereoisomer only a partial overlap of the carbazole ring systems is possible, as shown in Figure 6b. A certain rotation within a limited angle is possible, as shown by the temperature dependence of  $k_{DM}$ . <sup>1</sup>H NMR measurements, discussed above, showed the severe steric hindrance in *rac*-BCPe, which is evident in Figure 6b and accounts for the higher excimer emission energy.

**Quenching Effects in *rac*- and *meso*-BCPe.** As already mentioned above, the fluorescence emission is quenched by oxygen, as shown by the emission spectra in Figure 7, which were run on deaerated and air-saturated solutions. The difference in quenching

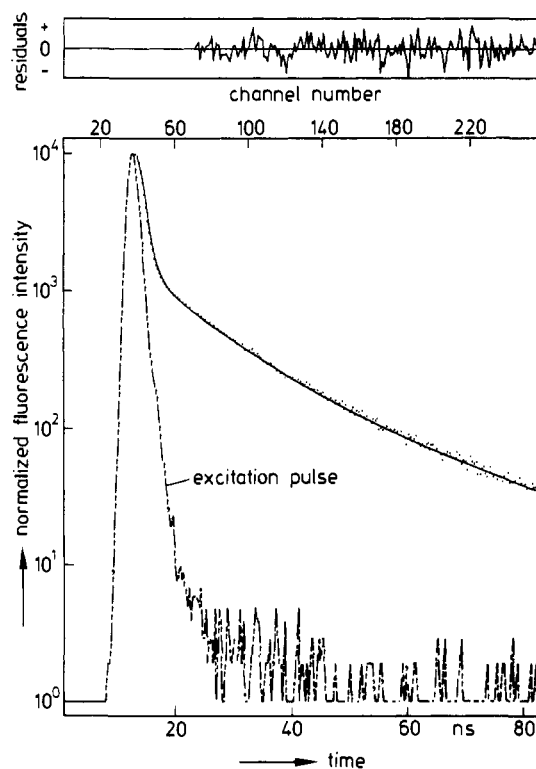


Figure 4. Monomer emission decay of *meso*-BCPe in deaerated solutions of MCH/ISP at  $\lambda_E = 347$  nm and 295 K.  $\lambda_{exc} = 300$  nm.

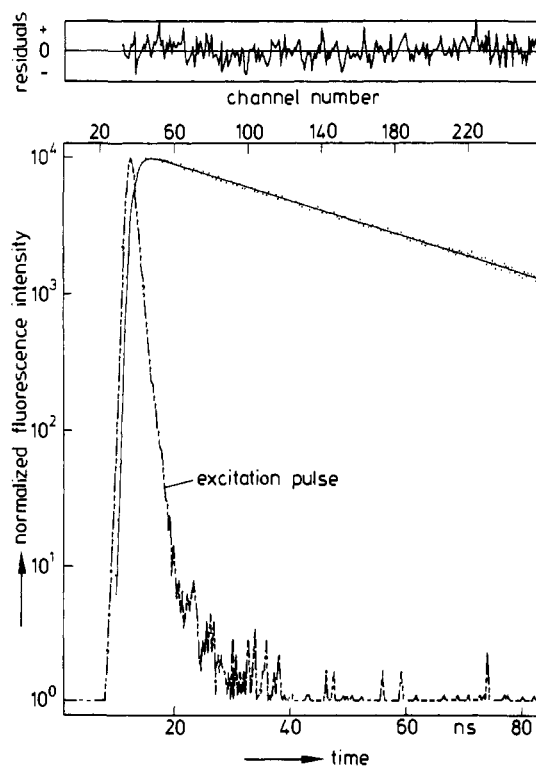


Figure 5. Excimer emission decay of *meso*-BCPe in deaerated solutions of MCH/ISP at  $\lambda_E = 347$  nm and 295 K.  $\lambda_{exc} = 300$  nm.

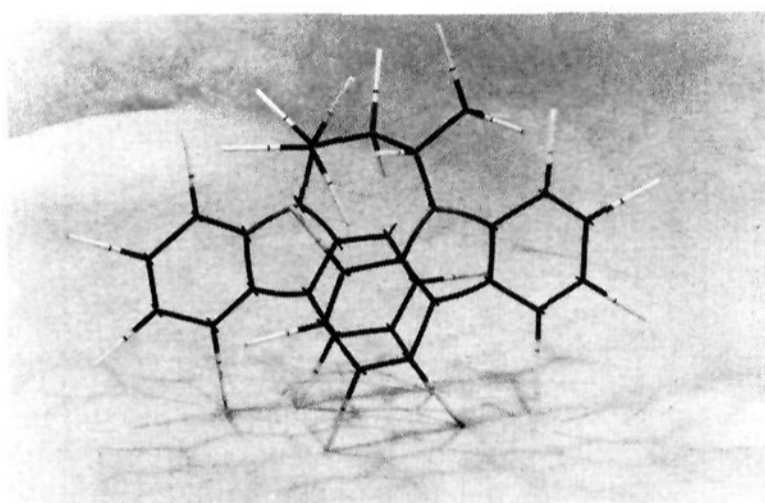
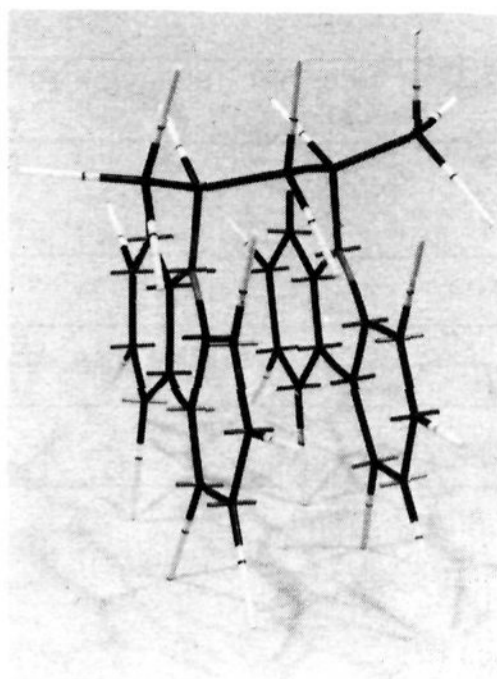


Figure 6. Molecular models of *meso*- (a) and *rac*-BCPe (b).

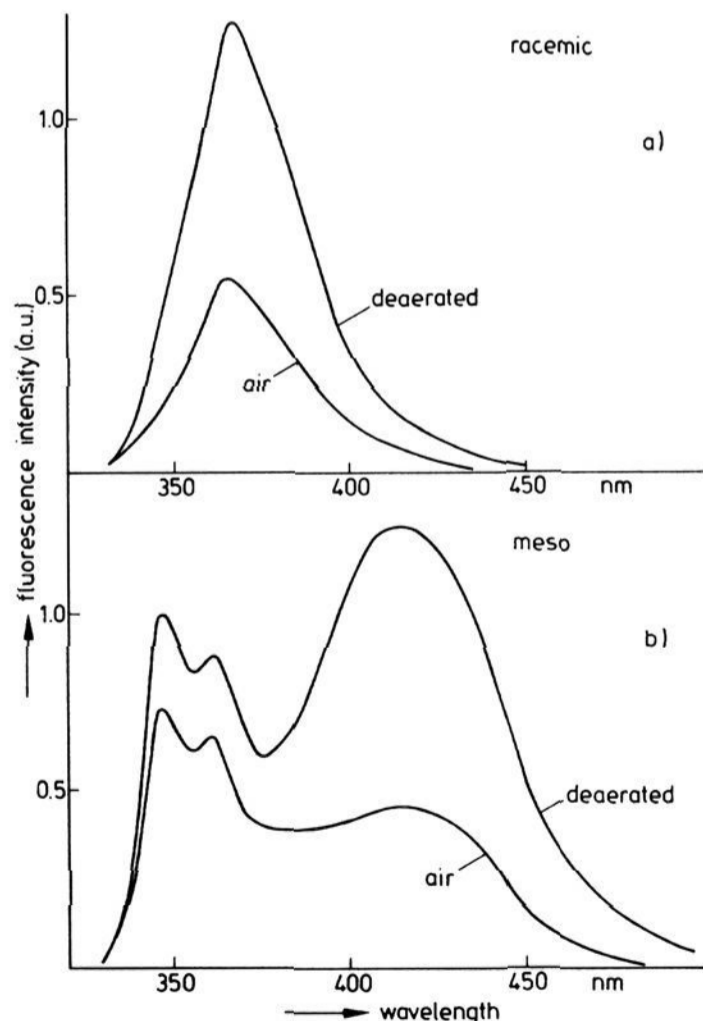


Figure 7. Spectral quenching of *meso*- and *rac*-BCPe in MCH/ISP at 295 K.

between the monomer and excimer emissions is due to the difference in rate constants. This quenching was studied more quantitatively by using dimethyl terephthalate (DMTP) instead of oxygen.

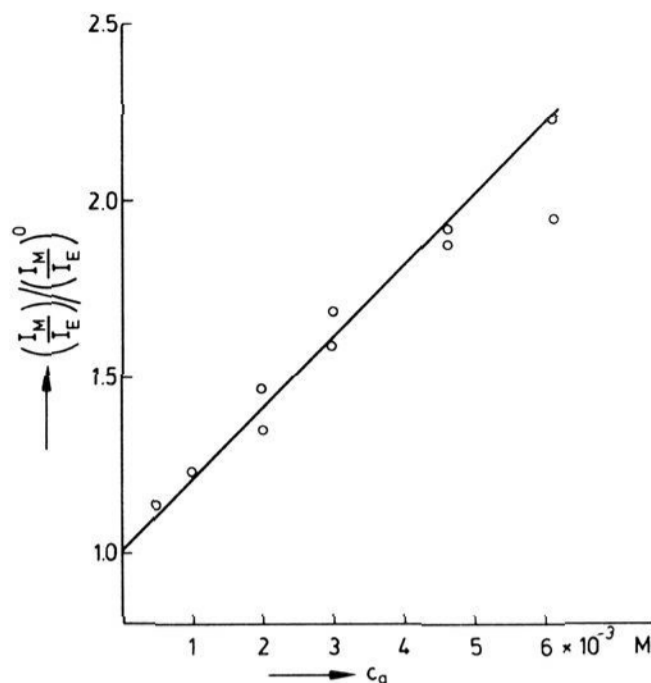


Figure 8. Stern-Vollmer plot for *meso*-BCPe in deaerated solutions of toluene. Quencher: dimethyl terephthalate.

With the assumption that both the monomer and excimer can be quenched, the solution to the corresponding rate equation yields the following results under photostationary state conditions:

$$\frac{I_M/I_E}{(I_M/I_E)^0} = 1 + \frac{k_q}{k_{MD} + k_D} c_q \quad (7)$$

in which  $(I_M/I_E)^0$  is the ratio of the monomer and excimer intensities in the absence of quencher,  $k_q$  is the second-order quenching rate constant, and  $c_q$  is the quencher concentration.

Quenching experiments were only performed with the *meso* diastereoisomer and the results are shown in Figure 8. From the slope of the line and using eq 7 we obtained  $k_{MD} + k_D = (4 \times 10^{-3})k_q$ .  $k_q$  can be derived from kinetic measurements as follows.

The decay processes after excitation of the molecules by a single laser pulse is given by eq 5 and 6 and the two rate constants  $\lambda_1$  and  $\lambda_2$ . According to the decay measurements  $\lambda_2 \ll \lambda_1$ , i.e.,

$$4(k_M k_D + k_D k_{DM} + k_M k_{MD}) \ll (X + Y)^2 \quad (8)$$

If the equation for  $\lambda_2$  is expanded as a series we have

$$\lambda_2^0 = \frac{k_M(k_D + k_{MD}) + k_D k_{DM}}{k_M + k_D + k_{DM} + k_{MD}} \quad (9)$$

Introducing the quenching rate constant we obtain

$$\lambda_2 = \frac{[k_M + k_q c_q][k_D + k_{MD} + k_q c_q] + [k_D + k_q c_q]k_{DM}}{k_M + k_D + k_{DM} + k_{MD} + 2k_q c_q} \quad (10)$$

Subtracting (9) from (10) we have

$$\lambda_2 - \lambda_2^0 = \frac{[k_M + k_D + k_{DM} + k_{MD} + k_q c_q]k_q c_q}{k_M + k_D + k_{DM} + k_{MD} + 2k_q c_q} \quad (11)$$

According to the results obtained in the previous section  $k_{DM}$  is about 2 orders of magnitude greater than  $k_M$ ,  $k_D$ , and  $k_{MD}$ . Thus if the quencher concentration is kept sufficiently low, so that  $k_q c_q \ll k_{DM}$ , eq 11 becomes

$$\lambda_2 - \lambda_2^0 \approx k_q c_q \quad (12)$$

Thus a measurement of the slow decay of the excimer emission is sufficient to determine  $k_q$ . Such measurements with and without DMTP as the quencher gave a  $k_q$  of  $9 \times 10^9 \text{ M}^{-1} \text{ s}^{-1}$ ; i.e., the quenching process is diffusion controlled. This  $k_q$  value can be also used to determine  $k_{MD} + k_D$ . From above  $k_{MD} + k_D = (4 \times 10^{-3})k_q$ , which yields a  $k_{MD} + k_D$  value of  $3.6 \times 10^7 \text{ s}^{-1}$ . This value was used in the previous section for determining various rate constants.

**Correlation between Excimer Formation in *rac*- and *meso*-BCPe with That in PVK.** It is useful to compare the emission spectra of *meso*- and *rac*-BCPe (Figures 1 and 2) with those obtained with

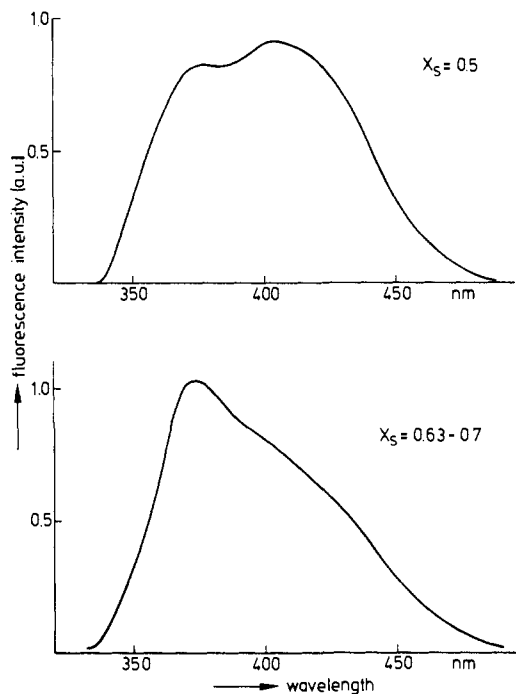


**Figure 9.** Emission spectra of PVK samples in deaerated solutions of 2-methyltetrahydrofuran (2-MeTHF) for samples with different syndiotactic diad mole fractions,  $X_s$ .

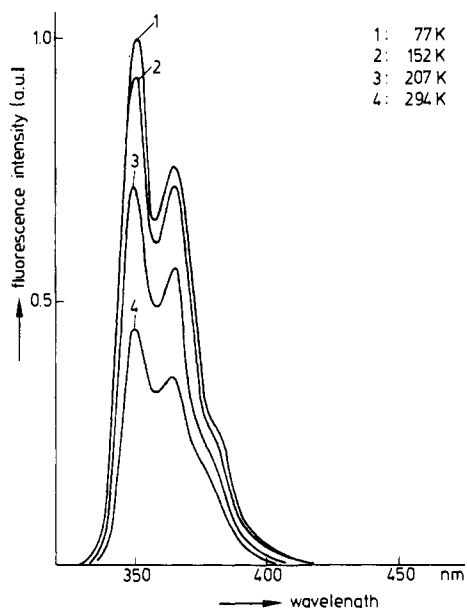


**Figure 10.** Emission spectra of *N*-ethylcarbazole in deaerated solutions of 2-MeTHF at various temperatures.

PVK (see Figure 9). The two spectra in Figure 9 were obtained with PVK samples with different mole fractions of syndiotactic and isotactic diads ( $X_s$  = syndiotactic diad mole fraction). From Figures 1, 2, and 9 it is evident that the emission of the *meso* excimer can be correlated with the long-wavelength peak in the emission spectrum of PVK (430 nm) and that of the *racemic* excimer with the short-wavelength peak (375 nm). The emission of ethylcarbazole is given in Figure 10 by way of comparison, only the typical monomer emission being present; i.e., excimers are not formed.

According to Figures 1 and 2 the emission spectra of *meso*- and *rac*-BCPe are strongly temperature dependent. It is interesting to note that the excimer emission of the *meso* diastereoisomer reaches a maximum at about room temperature (see Figure 3), whereas that of the *racemic* diastereoisomer passes through a maximum at much lower temperatures, i.e., at about 130 K. At

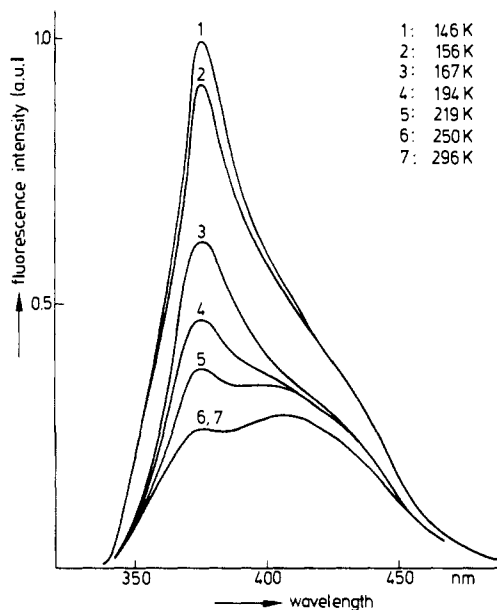


**Figure 11.** Emission spectra of PVK ( $X_s = 0.5$ ) in deaerated solutions of 2-MeTHF at various temperatures (146–296 K).

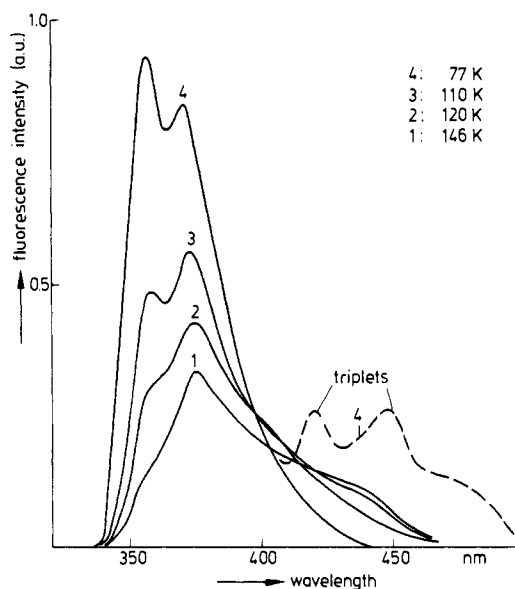


**Figure 12.** Emission spectra of PVK ( $X_s = 0.5$ ) in deaerated solutions of 2-MeTHF at various temperatures (146–77 K).

very low temperatures, below 80 K, no excimer emission was observed in both cases and the only usual monomer emission (345 and 363 nm) was observed.

For the sake of comparison, we have also measured the emission spectra of one PVK sample at different temperatures, as shown for two temperature ranges in Figures 11 and 12. If one compares these spectra with those for the BCPe diastereoisomers (Figures 1 and 2), one can see that in principle the same temperature dependence is observed in PVK as is found in the two diastereoisomers of BCPe.

These results clearly show the value of the model substances in unravelling the complexity of the PVK emission and also the degree of correlation between the excimer formation in PVK with that in the BCPe diastereoisomers.

**Assignment of Methine Peaks in the  $^{13}\text{C}$  NMR Spectrum of PVK and the Correlation between Excimer Intensities and  $^{13}\text{C}$  NMR Spectra for PVK.** A quantitative determination of the steric microstructure of PVK from the triad peaks corresponding to the methine group in the proton-decoupled  $^{13}\text{C}$  NMR spectrum of PVK requires that the *rr*, *mr*, and *mm* methine configurations relax to the same degree between rf pulses. However, for a given

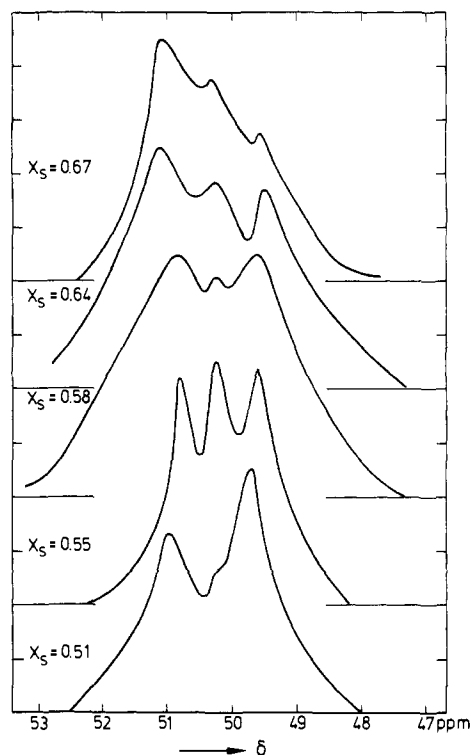


**Figure 13.** Proton-decoupled  $^{13}\text{C}$  NMR spectra of the methine group for several PVK samples with different syndiotactic dyad mole fractions  $X_s$ , prepared under different polymerization conditions. Measurements were carried out at  $+90^\circ\text{C}$  in dioxane.

sample of PVK under otherwise identical measurement conditions, the proton-decoupled  $^{13}\text{C}$  NMR spectrum of the methine group was found to depend upon the pulse angle. For example, fractional peak areas of 0.55, 0.21, and 0.24 were observed for a  $30^\circ$  pulse, which compared with 0.58, 0.23, and 0.19 for the corresponding peaks with a  $90^\circ$  pulse. Such deviations showed that the relaxation times of the three methine configurations were very different from one another, as has been previously observed for poly(methylmethacrylate)<sup>19</sup> and polypropylene.<sup>20</sup>

This explains the discrepancies between the  $^{13}\text{C}$  NMR spectra reported by Kawamura et al.<sup>21</sup> and ourselves for PVK samples prepared under similar conditions, since the results of Kawamura et al.<sup>21</sup> were obtained by using a  $45^\circ$  pulse and our results were obtained by using a  $90^\circ$  pulse and a delay of 30 s to ensure complete relaxation. In order to establish the conditions under which an undistorted methine spectrum could be observed for PVK with a  $90^\circ$  pulse, several experiments were carried out on the same sample of PVK with delays between pulses varying between 1.33 and 11.3 s. These clearly indicated that a delay of 10 s was sufficient to avoid distortion of the spectrum.

The habit of the proton-decoupled  $^{13}\text{C}$  NMR spectrum of the methine group was found to vary with the polymerization conditions, as first reported by Kawamura et al.<sup>21</sup> This is shown in Figure 13. The middle peak of the methine triad was identified as the mr peak by correlating the unspecified tacticities calculated with the assumption that the middle peak was the mr peak and that the other two peaks corresponded to the mm and rr peaks, with the glass transition temperatures for a series of PVK samples polymerized under various conditions.<sup>22</sup> The remaining two peaks were assigned on the basis of a comparison between the  $^{13}\text{C}$  NMR spectra of a series of PVK samples with increasing tacticity (see Figure 13) with the fluorescence emission spectra of the same series

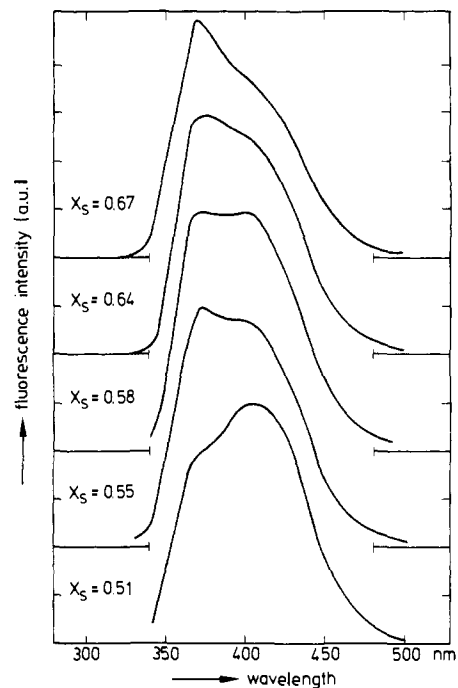


**Figure 14.** Fluorescence emission spectra for several PVK samples with different syndiotactic dyad mole fractions  $X_s$ , prepared under different polymerization conditions. Measurements were carried out in deaerated 2-MeTHF at room temperature.

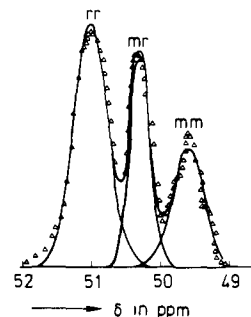


**Figure 15.** Proton-decoupled  $^{13}\text{C}$  NMR spectrum of the methine group of PVK, with the assignment of the triad peaks.

of PVK samples (see Figure 14). From this comparison it is evident that the intensity of the low-field peak in the methine triad increased as the intensity of the lower wavelength excimer increased. Since the latter had been assigned to a syndiotactic diad, the low-field peak must be the rr peak and the high-field peak must be the mm peak. This assignment of the triad peaks is shown in Figure 15.

This is at variance with the assignment of Williams and Froix<sup>23</sup> of the methine triads based on correlations with variations in the methylene proton intensities, which did not have the support of any independent data such as that presented here.

Finally, with the assumption that the fluorescence emission spectrum of PVK consisted of two components deriving independently from syndiotactic and isotactic diads, respectively, a curve-fitting analysis was carried out on the PVK fluorescence emission spectra feeding in the wavelength maxima observed for the long-wavelength fluorescence emission maxima of *rac*- and *meso*-BCPe. Figure 16 shows the correlation between the ratio of the integrated short-wavelength to long-wavelength components in the PVK fluorescence emission spectra and the ratio of the syndiotactic to isotactic diad mole fractions derived from the  $^{13}\text{C}$  NMR spectra for a series of PVK samples. The correlation can be seen to be quite good, when the potential errors in both the

(19) Lyerla, J. R.; Horikawa, T. T.; Johnson, D. E. *J. Am. Chem. Soc.* **1977**, *99*, 2463.

(20) Randall, J. C. *J. Polym. Sci., Part A-2* **1976**, *14*, 1693.

(21) Kawamura, T.; Matsuzaki, K. *Makromol. Chem.* **1978**, *177*, 2739.

(22) Terrell, D. R.; Evers, F.; Smoorenburg, H.; van den Bogaert, H. M. *J. Polym. Sci., Part A-2* **1982**, *20*, in press.

(23) Williams, D. J.; Froix, M. F. *Polymer Prepr., Am. Chem. Soc., Div. Polym. Chem.* **1977**, *18*, 445.

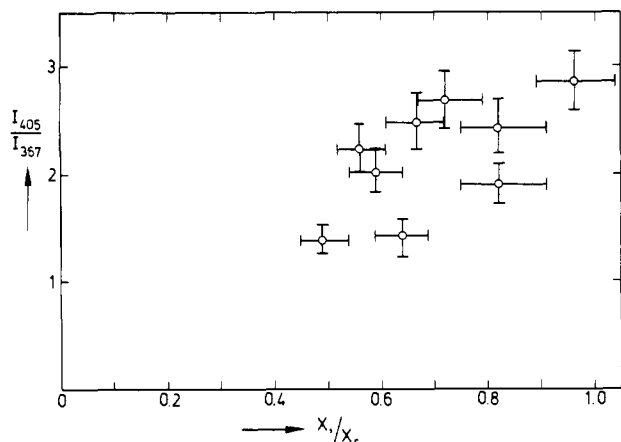


Figure 16. Dependence of  $I_{405}/I_{367}$  in the emission spectrum of PVK upon the ratio of isotactic and syndiotactic mole fractions,  $X_i/X_s$ .

measurement and analyses of the fluorescence and  $^{13}\text{C}$  NMR spectra are taken into account together with the reports that the fluorescence emission spectrum of PVK in fact consists of three components.<sup>24-26</sup> The third component was evidently sufficiently small so as not to invalidate the above analysis. One must conclude, moreover, that the two components of the fluorescence emission spectrum of PVK derive independently from syndiotactic and isotactic dyads, respectively. This is consistent with the absence of a photoemission point in the temperature dependence of the fluorescence emission of PVK observed by Johnson<sup>3</sup> and Roberts et al.<sup>27</sup> and with the kinetic schemes proposed by Roberts et al.<sup>24,25</sup> and Tagawa.<sup>26</sup>

### Conclusions

The excimers of *meso*- and *rac*-BCPe have been unambiguously correlated with the isotactic and syndiotactic diads in PVK. Furthermore the ca. 370- and ca. 420-nm excimer emissions in PVK could be directly correlated with the mole fractions of syndiotactic and isotactic dyads in PVK.

The rate constants for the excimer emissions for *meso*- and *rac*-BCPe have been quantitatively determined with photo-stationary-state emission and fluorescence decay measurements.

An assignment of the triad peaks in the proton-decoupled  $^{13}\text{C}$  NMR spectrum of the methine group of PVK has been made.

### Experimental Section

**Synthesis of *rac*- and *meso*-BCPe.** 2,4-Di(tosyloxy)pentane (DTPe) was prepared from a mixture of approximately equal quantities of *rac*- and *meso*-2,4-pentanediol (Fluka) as described by Eliel et al.<sup>28</sup>

***meso*-2,4-Di-*N*-carbazolypentane.** Sodium carbazole (0.1 mol) was dissolved in 200 mL of predried  $\text{Me}_2\text{SO}$  and a solution of 0.05 mol DTPe in 100 mL was added with stirring under dry nitrogen. After 3 $\frac{1}{2}$  h at room temperature the solution was poured into L of water under rapid stirring. The precipitate was filtered off, washed with water, dried, and recrystallized from ethanol to yield 3.5 g of *meso*-2,4-di-*N*-carbazolypentane with a melting point of 184 °C.

Anal. ( $\text{C}_{29}\text{H}_{26}\text{N}_2$ ) C, H, N. IR (KBr) 1595, 1485, 1455, 1330, 1315, 1225, 1215, 1160, 750, 727  $\text{cm}^{-1}$  [970  $\text{cm}^{-1}$  (vinyl) and 3420  $\text{cm}^{-1}$  (N-H) bands were absent]; UV (ethyl acetate) 260, 262, 287, 293, 327, 342 nm.

(24) Roberts, A. J.; Cureton, C. G.; Phillips, D. *Chem. Phys. Lett.* **1980**, *72*, 554.

(25) Roberts, A. J.; O'Connor, D. V.; Phillips, D. *Ann. N. Y. Acad. Sci.* **1981**, *366*, 109.

(26) Tagawa, S.; Washio, M.; Tabata, Y. *Chem. Phys. Lett.* **1979**, *68*, 276.

(27) Roberts, A. J.; Phillips, D.; Abdul-Rasoul, F.; Ledwith, A., to be submitted for publication. Reference 159 in: Ghiggino, K. P.; Roberts, A. J.; Phillips, D. *Adv. Polym. Sci.* **1981**, *40*, 69.

(28) Eliel, E. E.; Hutchins, R. O. *J. Am. Chem. Soc.* **1969**, *91*, 2703.

The *meso* isomer was identified by the similarity of its  $^1\text{H}$  NMR spectrum to that of *meso*-2,4-diphenylpentane<sup>17</sup> and the invariant nature of the spectrum in the presence of chiral shift reagents.

**1,2,3,4,10,11-Hexahydrocarbazole (HHC)** was prepared from 1,2,3,4-tetracarbazole (THC) according to the method of Borsche.<sup>29</sup>

**2,4-Bis(*N*-1,2,3,4,10,11-hexahydrocarbazolyl)pentane (BHHCPe)** was prepared by melting 0.23 mol of HHC at 110 °C and then adding 0.056 mol of DTP. Over a period of 1 $\frac{1}{2}$  h the temperature was increased to 160 °C and then the mixture was heated under reflux for 3 h. After the melt was neutralized with sodium carbonate solution and the excess HHC steam distilled off, the resulting oil was extracted with dichloromethane, the extract dried, and the solvent evaporated. The residue was purified on a basic alumina column, by elution with a 2:1 by volume mixture of *n*-hexane and benzene. The first fraction was BHHCP in a yield of 27%.

Anal. ( $\text{C}_{29}\text{H}_{38}\text{N}_2$ ) C, H, N.  $^1\text{H}$  NMR  $\delta$  1.1-1.3 ( $\text{CH}_3$ ), 1.3-1.8 ( $\text{CH}_2$  ring), 1.8-2.4 ( $\text{CH}_2$  chain), 3.0-3.2 (CH), and 6.4-7.2 (aromatic). IR (oil) 2930, 2860, 1610, 1480, 1460, 750, 737, 680  $\text{cm}^{-1}$ .

***meso*- and *rac*-BCPe** were prepared from BHHCPe by use of chloranil in xylene under reflux by using the method of Barclay et al.,<sup>16</sup> in a yield of 6.5%. This was shown by  $^1\text{H}$  NMR,  $^{13}\text{C}$  NMR and HPLC to contain ca. 50% of the racemic isomer.

Anal. ( $\text{C}_{29}\text{H}_{26}\text{N}_2$ ) C, H, N.

**Separation of *meso*- and *rac*-BCPe.** A Pye Unicam liquid chromatograph with a LC3 UV detector, preparative and analytical columns of Partisil 10, and an eluting medium of 95:5 by volume *n*-hexane to diethyl ether were used to separate the isomers. The racemic and *meso* isomers were found to have retention volumes of 23.5 and 29.2 mL, respectively, at room temperature, by use of a preparative column with an internal diameter of 9.4 mm. The racemic isomer was identified by the similarity of its  $^1\text{H}$  NMR spectrum to that of *rac*-2,4-diphenylpentane.<sup>4</sup>

**NMR Measurements on *meso*- and *rac*-BCPe.**  $^1\text{H}$  NMR measurements were carried out in deuteriochloroform at room temperature or in 1,2-dibromoethane- $d_4$  at 110 °C on a 270-MHz Bruker spectrometer. The  $^{13}\text{C}$  NMR spectra were run on a 90-MHz Bruker spectrometer or a 100-MHz Varian XL 100 FT spectrometer and were carried out in dioxane solution at 60 °C.

**$^{13}\text{C}$  NMR Measurements on PVK.**  $^{13}\text{C}$  NMR measurements were carried out either on a Varian XL-100-12 FT spectrometer or on a Bruker 270-MHz spectrometer. Perdeuteriodioxane (Merck) was used as the solvent and the measurements were carried out at +90 °C, as suggested by Kawamura et al.<sup>21</sup> The resolution of the  $^{13}\text{C}$  NMR and fluorescence emission spectra were further improved by computer curve fitting, with the assumption that the peaks had Gaussian distributions.

**Fluorescence Emission Measurements.** Fluorescence measurements were carried out in deoxygenated *n*-hexane or 2-methyltetrahydrofuran solution at room temperature with a UV lamp with a broad-band filter ( $\lambda_{\text{max}} \approx 280$  nm) as the excitation source and a monochromator with a photomultiplier as detector. The fluorescence decay was measured by a pulse nanosecond fluorometer, System 3000 (PRA). This fluorometer, based on time-correlated single photon counting, was directly connected to a computer that was used for determining the rate constants for one- and two-exponential decay of the fluorescence intensities. This technique made it possible to determine the rate constants with excellent precisions as proved by measurements with other systems.<sup>30,31</sup> The stabilizer was removed from the 2-methyltetrahydrofuran before use.

**Acknowledgment.** We are indebted to Dr. Sinnwell (Hamburg University), Dr. Moser (Unilever Forschungslaboratorium, Hamburg) and H. M. van den Bogaert and H. Smoorenburg (Philips Natuurkundiglaboratorium, Eindhoven) for carrying out the NMR measurements and to Dr. M. Bühring (Amco, GmbH, Tornesch) for measuring the fluorescence lifetimes. We are also grateful for valuable discussions with Dr. D. C. Sherrington (University of Strathclyde) and Dr. C. P. Klages of this laboratory.

**Registry No.** *meso*-BCPe, 80039-86-7; ( $\pm$ )-BCPe, 80039-85-6; DTPe, 35196-66-8; BHHCP, 86471-83-2; HHC, 1775-86-6; PVK, 25067-59-8; sodium carbazole, 7395-04-2.

(29) Borsche, W.; Witte, A.; Bothe, W. *Liebigs Ann. Chem.* **1908**, *359*, 49.

(30) Memming, R.; Kobs, K. *J. Phys. Chem.* **1981**, *85*, 2771.

(31) Memming, R.; Kobs, K. *Chem. Phys. Lett.* **1981**, *80*, 475.